The *Arabidopsis* myc/bHLH gene *ALCATRAZ* enables cell separation in fruit dehiscence

Sarojam Rajani*† and Venkatesan Sundaresan*‡

Background: Several processes of plant development, such as abscission, pollen release, fruit dehiscence, and seed dispersal, require organs or tissues to physically disassociate or split open. Due to the immobility of plant cells, these processes occur through coordinated mechanisms of cell separation that are not found in animals. *Arabidopsis* produces dry dehiscent fruits (siliques) making it a convenient system for the genetic study of cell separation associated with dehiscence.

Results: We describe here a novel mutation in *Arabidopsis* called *alcatraz* (*alc*), which prevents dehiscence of fruit by specifically blocking the separation of the valve cells from the replum. The *ALC* gene is shown to encode a protein related to the myc/bHLH family of transcription factors and is expressed in the valve margins of the silique, which is the site of cell separation during dehiscence. Detailed studies using TEM indicates that *ALC* enables cell separation in *Arabidopsis* fruit dehiscence by promoting the differentiation of a strip of labile nonlignified cells sandwiched between layers of lignified cells. Transgenic plants expressing antisense or dominant-negative *ALC* are defective in silique dehiscence.

Conclusions: Cell separation in fruit dehiscence requires a specialized cell layer which is nonlignified and capable of autolysis, specified by a myc/bHLH protein encoded by *ALC*. These findings may have relevance to other processes requiring cell separation, as well as for the practical design of crops with reduced seed losses.

Addresses: *Institute of Molecular Agrobiology and †Department of Biological Sciences, 1 Research Link, The National University of Singapore, Singapore 117604, Singapore. ‡Section of Plant Biology and Department of Agronomy, University of California, One Shields Avenue, Davis, California 95616, USA.

Correspondence: Venkatesan Sundaresan
E-mail: sundar@ucdavis.edu

Received: **4 September 2001**
Revised: **11 October 2001**
Accepted: **11 October 2001**

Published: **11 December 2001**

Current Biology 2001, 11:1914–1922

0960-9822/01/$ – see front matter

Background

In many flowering plants, completion of the reproductive cycle by seed dispersal occurs through a process called "fruit dehiscence," in which the fruit opens and releases the seeds. This process is accomplished through a coordinated program of cell separation, a feature shared with other processes, such as abscission, anther dehiscence, and root growth, wherein tissues or organs must disjoin or split open [1]. *Arabidopsis* provides a suitable system for the genetic study of this process. It produces dry dehiscent fruits known as "siliques" that develop from a fertilized gynoecium. The gynoecium in *Arabidopsis* consists of two congenitally fused carpels creating a single ovary, which is topped with a short style and stigma [2]. The septum is the fused tissue that the two carpels share, and it internally divides the ovary. The replum constitutes the outer margin of the septum. The carpel walls are known as the valves, which are joined to the replum. After fertilization, the gynoecium develops to form the silique [3].

Dispersal of seed occurs through dehiscence, which consists of a programmed series of events by which the valves separate from the replum releasing the seeds. This process requires the prior development of the dehiscence zone (DZ), which is formed at the valve margin. The valve margin consists of a narrow band of cells about four cell files, at the valve replum boundary extending the entire length of the fruit. During silique expansion, the valve margin cells expand more slowly than valve cells, resulting in noticeable constriction at the valve margin. The DZ is derived from the valve margin cells and consists of both lignified and unlignified cells [4]. Out of the two internal valve cell layers, En*a* and En*b*, the lignification of En*b* layer also contributes toward dehiscence (Figure 1). After the lignification of En*b*, the En*a* starts degrading. As the fruit dries, differential shrinkage between the thin-walled nonlignified cells of the valve and the rigid lignified En*b* cells is believed to create mechanical tensions in the silique, which acts in a spring-like manner. As the fruit matures (stage 18 of flower development) [5], a discrete group of cells within the DZ undergo middle lamella breakdown, and, concomitantly, the existing tension in the silique allows valve detachment from the replum ensuing seed dispersal [6].

In *Arabidopsis*, two closely related MADS-box genes have been identified, *SHATTERPROOF1* (*SHP1*) and *SHATTERPROOF2* (*SHP2*), which are required for fruit dehiscence. *SHP1* and *SHP2* are functionally redundant, as

Figure 1

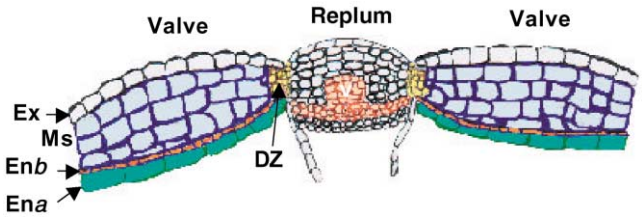

Schematic representation of transverse section at the replum valve region. The exocarp (Ex), mesocarp (Ms), the two endocarp layers Ena and Enb, and the replum vasculature (V) are shown. The dehiscence zone (DZ) forms at the valve replum boundary.

single mutants do not exhibit any abnormal phenotype. In contrast, *shp1 shp2* double mutant produces indehiscent fruits. Analysis of *shp1 shp2* fruit has revealed the absence of dehiscence zone and reduction in lignification of the valve margin cells. Hence, *SHP1* and *SHP2* are required for the proper development of fruit valve margins, including dehiscence zone differentiation and lignification [7]. Another MADS-box gene called *FRUITFULL* is responsible for specifying a valve cell fate during carpel and fruit development [8]. In *ful* mutants, the siliques do not elongate after fertilization and remain short. Recently, it has been shown that *FUL* negatively regulates *SHP1SHP2* expression, and constitutive expression of *FUL* leads to the absence of DZ because valve margin cells adopt a valve cell fate. Consequently, the 35S::*FUL* gain-of-function plants produce indehiscent fruits [9]. However, the genetic control of the actual process of cell separation, which results in the physical dissociation of valve and replum, has remained obscure. The identification and characterization of genes that control this step is important not only for understanding the mechanism of fruit dehiscence but also can lend insights into the general mechanisms underlying cell separation in plant development. Finally, knowledge of the genetic control of this process is of potential agronomical importance, since premature dehiscence or pod shatter leads to significant losses in crops, such as canola.

In this study, we describe a recessive mutant in *Arabidopsis*, named *alcatraz* (*alc*), that disrupts the process of silique dehiscence. *ALC* was cloned using the *Ds* gene trap element as a tag, and it encodes a myc/bHLH protein. Both lignification and external appearance of DZ remains unchanged in *alc*. We show that *alc* plays a key role in cell separation during fruit dehiscence by promoting the differentiation of a cell layer that is the site of separation between the valves and the replum with in the DZ.

Results

Identification and mutant phenotype of *alcatraz*

The *alc* mutation was isolated from a collection of independent insertion lines generated using the *Ds* gene trap transposons as described in Sundaresan et al. [10]. Backcrossing to wild-type Landsberg *erecta* plants confirmed that *alc* segregates as a single recessive mutation. The abnormal phenotype is observed in the siliques, which are indehiscent. In wild-type plants, by stage 19 [5], the silique begins to turn yellow, and slowly the valves separate from the replum releasing the seeds. In contrast to those of wild-type plants, *alc* siliques do not dehisce. Mutant siliques elongate and turn yellow, but valve separation from the replum fails to occur (Figure 2a,b). The seeds can be harvested only if the siliques are opened manually by the application of pressure at the valve margins. Earlier events of development, like vegetative growth, floral development, floral organ senescence, and anther dehiscence, are not detectably different from wild-type plants.

Since DZ formation at the valve margin and lignification of the internal valve layer is known to be important for dehiscence, we examined the development of the DZ and lignification pattern in homozygous *alc* siliques. Scanning electron microscopy (SEM) studies revealed that the external appearance of the DZ in the mutant siliques at stage 17–18 is not detectably different from that of wild-type siliques. The constriction at the valve margin region looks normal as seen in the wild-type (Figure 2c,d). In contrast, SEM of *shp1 shp2* siliques shows the absence of the DZ, and the constriction of the valve margin is far less defined when compared to wild-type [7].

The lignification pattern of *alc* siliques was determined using phloroglucinol, a lignin-specific histological stain. No change in the lignification pattern was observed. Valve margin cells comprising the lignified cells (LC) of the DZ and the internal valve layer is lignified in *alc* siliques (Figure 3a,b). Together, these data indicate that the DZ formation as observed externally by SEM and lignification pattern is not disrupted in the *alc* mutant.

The *alc* mutation fails to differentiate a nonlignified cell layer at the site of separation

In view of the absence of any external visible defects, the internal cellular anatomy of the DZ of *alc* and wild-type stage 17/18 siliques was examined by performing transverse sections. This revealed abnormalities in the DZ of *alc* siliques, which appeared to be due to the absence of a layer of nonlignified cells (NLC) found in wild-type siliques between the LC of the DZ and the cells of the replum (Figure 3c,d). To view the DZ at an ultrastructural level, transmission electron microscopy (TEM) was performed on transverse sections of wild-type and mutant siliques. Lignified cells can be identified by their thick cell walls under TEM, and the different cell types can be clearly distinguished.

Wild-type siliques show a row of small isodiametric non-

Figure 2

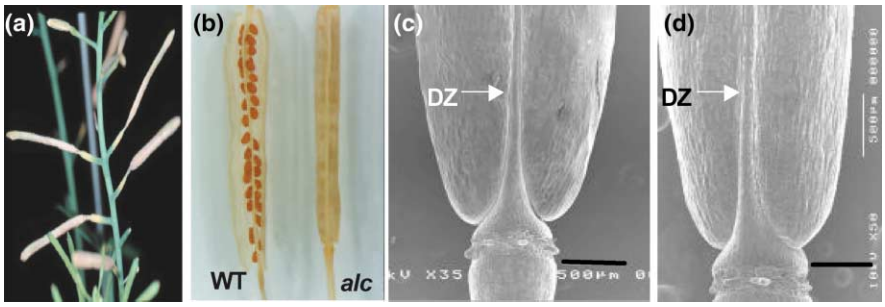

(a) Mutant phenotype of *alc* plants where siliques fail to dehisce. **(b)** A comparison of wild-type and *alc* siliques at maturity. **(c,d)** SEM analysis of DZ differentiation in (c) wild-type and (d) *alc* siliques at stage 17. Scale bars in (c,d), 500 μm.

lignified cells that form the NLC layer sandwiched between the LC of the DZ and replum cells (Figure 4a). Toward the inner valve margin, this NLC layer separates the lignified cells of the DZ and the lignified internal valve layers from the lignified replum vasculature. TEM shows that the degradation of En*a* cells is not complete in the wild-type: a few cells remain at the inner valve margin, which are later lignified. The separation of the lignified cells at the inner valve margin and replum is maintained by two to three cells of the NLC layer, even in later stages where further lignification of En*b* and remaining En*a* cells is known to occur. TEM of wild-type siliques at stage 19 shows a clear separation of the valves and the replum by the dissolution of the NLC, which is no longer identifiable. Intact cells of the LC layer and the replum are seen remaining attached to the fracture faces (Figure 4b).

TEM of *alc* siliques shows that the cells present at the NLC position have a different morphology: they appear to be bigger in size, especially toward the inner valve margin (Figure 4c). At stage 18, where further lignification is known to occur, these abnormal cells present at the inner valve margin also become lignified (Figure 4d). These ectopically lignified cells (ELC) create a lignified bridge between the lignified inner valve cell layers and the lignified replum vasculature (Figure 4d,e). TEM of mature yellow *alc* siliques reveals that cells toward the outer valve margin have degraded, as indicated by the asterisk (Figure 4e). However, this separation observed in *alc* is not as smooth as seen in wild-type, where intact cells constitute the fracture faces, suggesting that separation is accomplished by cell rupture rather than dissolution. This degradation was visible externally by SEM as grooves between the valve and the replum, as indicated

Figure 3

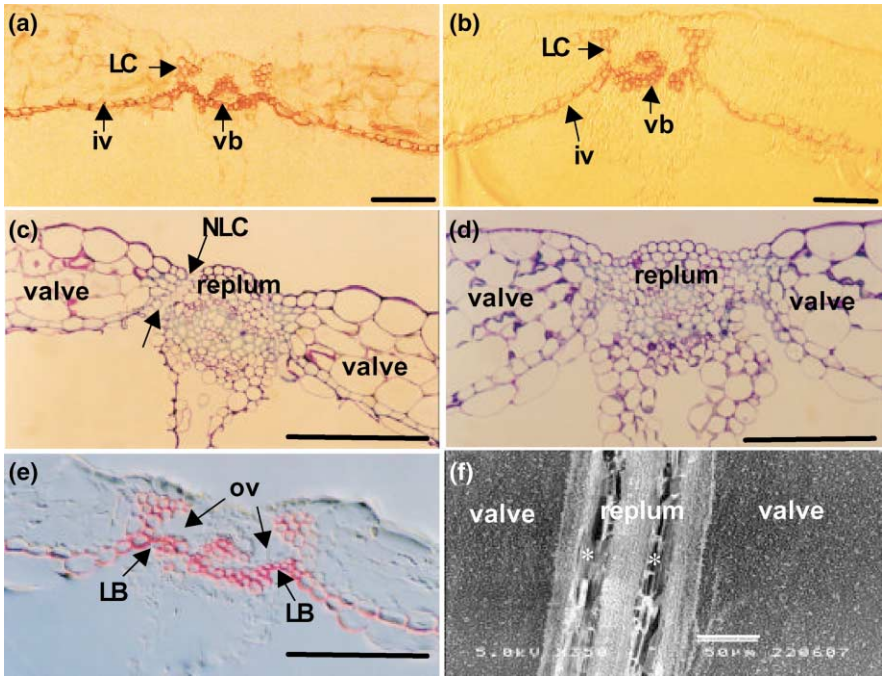

Transverse sections of **(a,c)** wild-type and **(b,d)** *alc* siliques at stage 17 silique. (a,b) Stained with phloroglucinol. Lignification of the LC layer of DZ, of the internal valve cell layers (iv), and the vascular bundle (vb) of the replum is not affected in *alc*. (c,d) Stained with Toluidine blue, showing the defect in the formation of NLC in the DZ of *alc*. **(e)** Transverse section of indehiscent *alc* silique (stage 18/19) stained with phloroglucinol, showing the lignified bridge (LB) between the valve and the replum, toward the inner valve margin and degraded cells at the outer valve margin (ov). **(f)** SEM of indehiscent *alc* silique (stage 18/19) showing the external degradation of outer valve margin cells at the DZ, indicated by the asterisks. Scale bars in (a–e), 100 μm; in (f), 50 μm.

Figure 4

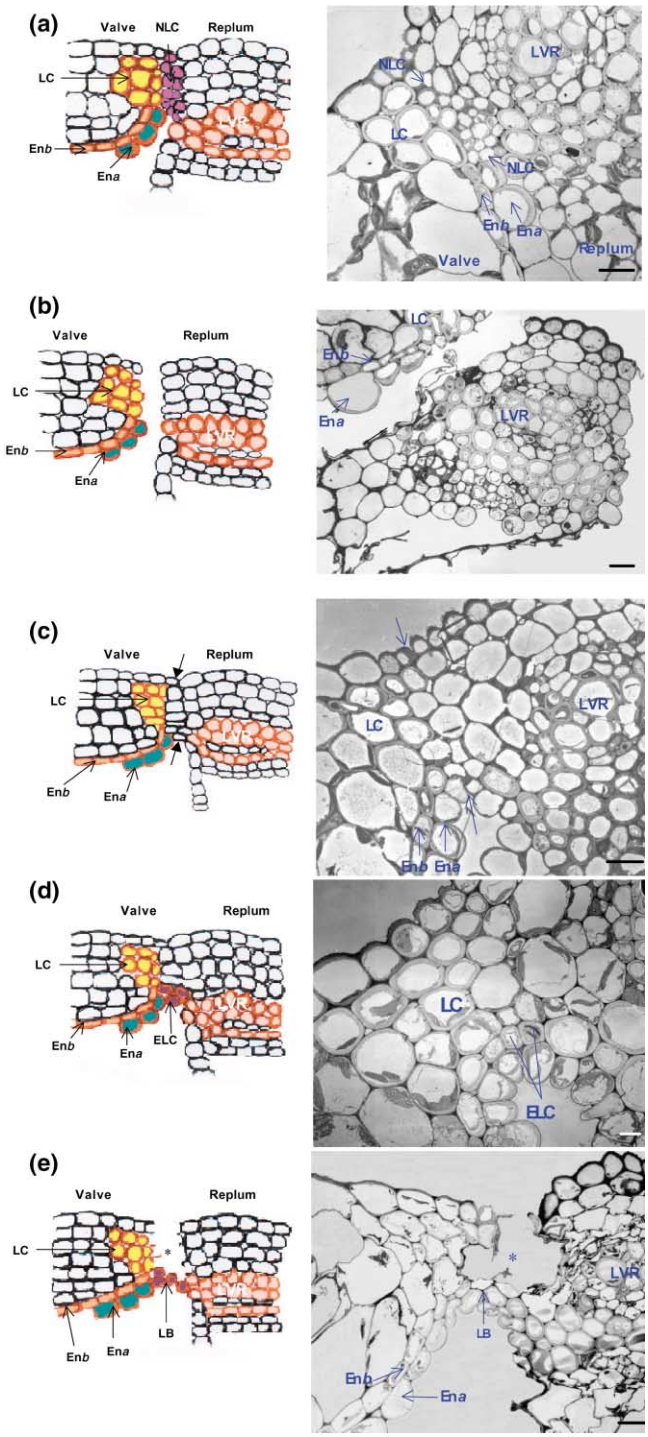

Schematic representation and TEM showing the anatomy of the dehiscence process at the valve replum boundary. Transverse sections of **(a,b)** wild-type silique and of **(c–e)** *alc* silique. (a,c) Late stage 17 siliques showing the DZ and surrounding tissues; arrows indicate the position of formation of the NLC in DZ in the wild-type and its absence in the mutant. In wild-type, the NLC separates the lignified inner valve margin cells En*a* and En*b* from the LVR. (d) Stage 18 silique (higher magnification) showing the ectopically lignified cells (ELC) bringing the En*a* and En*b* layer in continuity with the LVR at the inner valve margin. (b,e) Stage 18/19, in the wild-type, the valve is completely detached from the replum, and intact cells remain attached to both fracture faces; in *alc*, the valve and replum are held together by the lignified bridge (LB). NLC, nonlignified cells of the DZ; LC, lignified cell layer of the DZ; and LVR, lignified vasculature of the replum. Scale bars, 5 μm.

by asterisk in Figure 3f. At the inner valve margin, the valves and the replum are seen held together by the lignified bridge. Additional confirmation of lignified bridge was obtained by light microscopy of transverse section of indehiscent siliques stained with phloroglucinol (Figure 3e). We conclude that this lignified bridge of cells prevents silique dehiscence in *alc* mutants.

The *ALC* gene encodes a putative transcription factor of the myc/bHLH family

Southern blot analysis of genomic DNA revealed that the mutant plant carries a single transposed *Ds* element (data not shown). Genomic sequences flanking the *Ds* element in the *alc* mutant were obtained by TAIL PCR [11] and sequenced. A BLAST [12] search with the *Arabidopsis* database revealed that the flanking sequences were identical to the genomic sequence from chromosome 5 contained within a TAC clone: K21H1. The *Ds* element had inserted in a gene encoding a predicted protein (AT5g67110). A probe spanning the insertion site was used to screen a floral cDNA library. All the cDNA clones isolated from the screen had a length of 931 bp and were predicted to encode a 210 amino acid protein. The assignment of the putative translational initiation codon (ATG) was confirmed by 5′ RACE-PCR (data not shown). Alignment of the genomic and cDNA sequences shows that the gene contains five exons, and the *Ds* element has inserted at the beginning of third exon (Figure 5a). RT-PCR analysis shows the absence of *ALC* mRNA in siliques of homozygous mutant plants, indicating that the *Ds* insertion results in a null allele (Figure 6a).

A profile scan output for ALC protein predicted a bHLH motif at the C terminus and a bipartite nuclear localization signal at positions shown in Figure 5b. The *Ds* insertion results in the disruption of the bHLH domain. bHLH proteins, typified by the mammalian oncoprotein myc, are known to function by binding DNA through their basic domain and dimerizing by means of their helix-loop-helix region. Database searches revealed that the ALC protein belongs to the broad range of myc-bHLH-related proteins from plants and animals. It has closest homology with two *Arabidopsis* bHLH proteins, SPATULA [13] and PIF3 [14], and the maize regulatory R proteins [15]. The sequence relationship among known myc-related bHLH proteins with ALC is illustrated in Figure 5c. At 210 amino acids, ALC is a much smaller protein when compared to other myc-related proteins in plants, which are typically

Figure 5

(a) Schematic drawing of the *ALC* gene, showing the *Ds* insertion site at the beginning of the third exon. The exons are shown as boxes and the introns as lines. **(b)** Amino acid sequence of ALC predicted protein. The bHLH domain is underlined, and the NLS-BP is at amino acid position 90–107. **(c)** Alignment of the bHLH region amino acid sequence of ALC with other related proteins, namely, *Arabidopsis* SPATULA [13], *Arabidopsis* PIF3 [14], *Arabidopsis* rd22BP1 [17], *Arabidopsis* ATMYC [32], maize B-Peru [33], and maize Lc [34]. **(d)** The genomic sequence and amino acid sequence flanking the *Ds* insertion site and the footprint analysis. (1) Region of wild-type *ALC* locus and the amino acid sequence coded by this region prior to *Ds*G insertion. (2) Sequence alteration at *ALC* locus after *Ds* insertion. Nucleotides in bold represent the bases added during *Ds* insertion. (3) The 9 bp footprint (bold) seen after *Ds* excision in the revertant, which results in the addition of three amino acids (bold) in the protein and (4) 10 bp footprint (bold) seen in the stable allele, which results in a frameshift. The changes in the amino acid sequence are italicized.

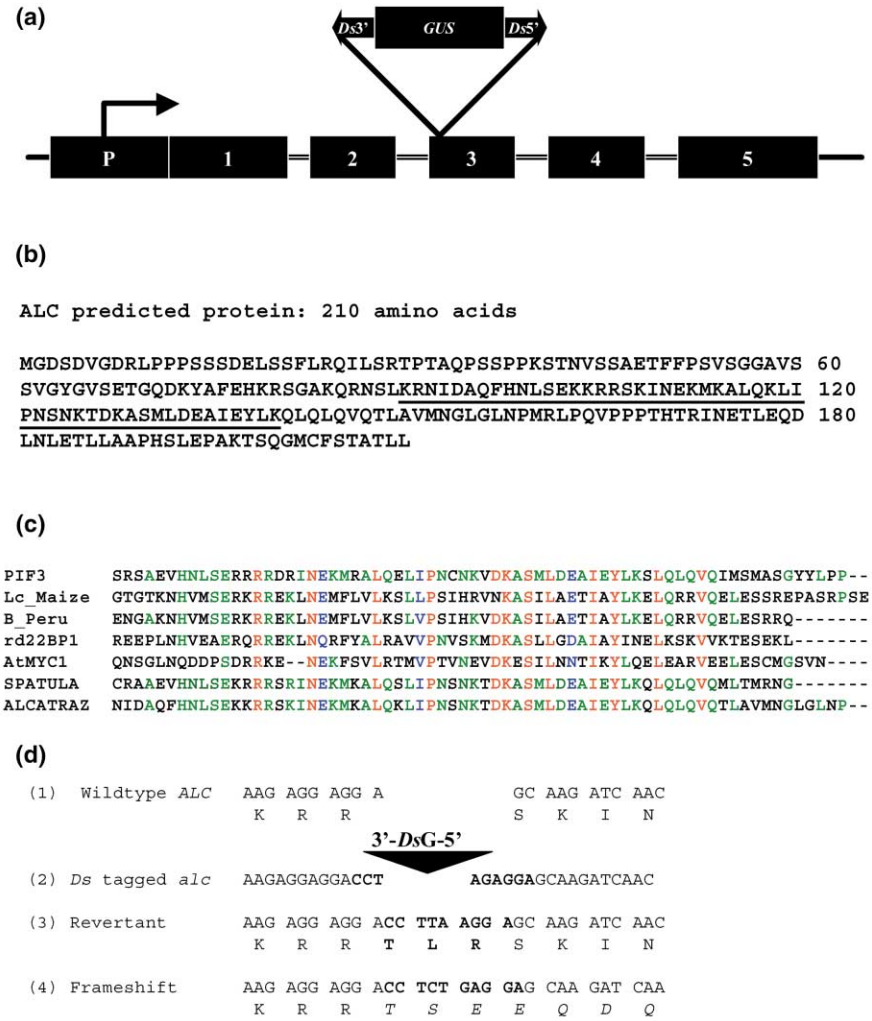

larger than 500 amino acids. Most known plant bHLH proteins also exhibit homology outside the bHLH domain, such as the myb-interacting domain of the R proteins [16, 17] or the PAS domain of the PIF-3 protein [18]. While such conserved domains are not observed in ALC, it may be capable of association with other myc-related proteins by heterodimerization using the HLH domain.

Figure 6

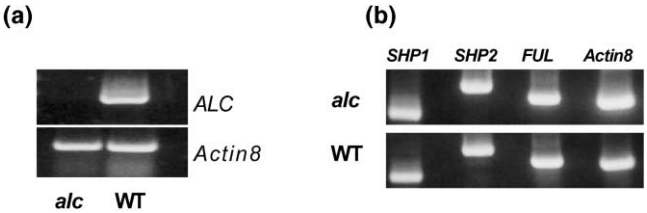

RT-PCR analysis. **(a)** *ALC* and *Actin8* (control) RNA in *alc* mutant and wild-type siliques. **(b)** RNA expression of *SHP1*, *SHP2*, *FUL*, and *Actin8* (control) in *alc* and wild-type siliques.

To confirm that the observed phenotype was caused by the insertion of the *Ds* element into the *ALC* gene, *Ds* was remobilized by crossing to plants expressing *Ac* transposase, and eight independent revertants were generated in which dehiscence was restored. The *Ds* insertion-generated sequence changes in the *ALC* gene are shown in Figure 5d. All sequenced revertant alleles contained a 9 bp footprint at the site of the *Ds* excision, resulting in the addition of three amino acids to the original protein (Figure 5d). In addition, a stable frameshift allele with 10 bp footprint was also isolated in which the plants remained indehiscent (Figure 5d). A mutant with a similar phenotype and with a mutation in the same gene was independently identified (M. Yanofsky, personal communication).

Figure 7

(a)

GATGACGGCG GAGCTGTTTC TTCCGTCGGT TATGGAGTCT CTGAAACTGG CCAAGACAAA
TATGCTTTCG AACACAAGAG AAGTGGAGCT AAACAGAGAA ATTCGTTGAA GAGAAACATT
GATGCTCAAT TCCACAACTT GTCTGAAAAG GTTATATGCA GGTCC*atg*GT CCGTCCTGTA
GAAACCCCAA CCCGTGAAAT CAAAAAACTC GACGGCCTGT GGGCATTCA

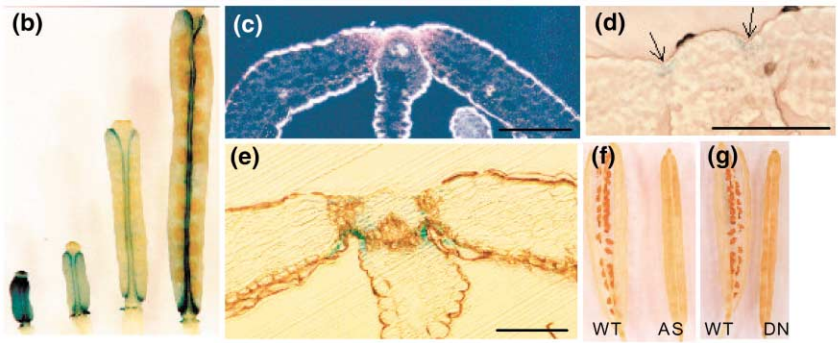

GUS analysis. **(a)** mRNA-*GUS* fusion analysis by RT-PCR. The underlined sequence represents the *GUS* gene; the *GUS* ATG is italicized. GUS histochemical localization **(b)** in the developing carpels of *alc* mutants, **(c)** in crosssections of silique at early stage 17 of *alc*/+ plants (dark field), **(d)** in crosssections of silique at late stage 17 of *alc*/+ plants, arrows indicate weak GUS staining, **(e)** in crosssections of silique at late stage 18 in *alc* mutants. Indehiscent phenotype observed in wild-type plants transformed with **(f)** *ALC* antisense construct and **(g)** *ALC* dominant-negative construct. AS, antisense plant; DN, dominant-negative plant. Scale bars, 100 μm.

ALC is expressed at the valve margins of the silique

Since the gene trap *Ds* element carries a *GUS* reporter gene, it was possible to analyze the endogenous gene expression pattern by staining for *GUS* activity. RT-PCR and sequencing of the fusion transcript confirmed that the *GUS* gene ATG is in frame with the *ALC* gene (Figure 7a). The intensity of *GUS* staining in the heterozygous plants is very much reduced when compared to the homozygous plants, but the expression pattern is similar. In the adult plant, prior to fertilization, *GUS* activity is diffused throughout the gynoecium but intense at the valve margin and in stigmatic papillae. After fertilization, the expression becomes restricted to valve margin region (Figure 7b). In sections at early stage 17, *GUS* expression is seen in a broad area comprising the valve margin cells and replum epidermis (Figure 7c). But, at late stage 17, the expression becomes more confined to cells within the DZ, with more intense expression toward the outer valve margin (Figure 7d). Since *GUS* expression in heterozygous plants is very weak at this stage, thick sections were required to visualize the *GUS* expression. As this reduces the clarity of the cell morphology, it is not clear whether the expression becomes restricted to the NLC layer. Sections of *alc* mutant siliques at stage 18/19 show that the expression is strongest in the cells that will form the lignified bridge present at the inner valve margin, which holds the valve and replum together (Figure 7e). The *GUS* expression pattern of these late stages could not be obtained in the heterozygous plants, because the valve separated from the replum during sectioning.

The expression of *ALC* at the valve margins and the DZ during silique dehiscence is consistent with its presumptive role as a transcriptional activator of dehiscence. Although the effect of the mutation is restricted to dehiscence, *ALC* is also expressed in other organs and developmental stages. *GUS* expression is observed diffusely in the ovules at various stages of development: in the nectaries, the fruit pedicel branching point, the vasculature of cotyledons, in newly emerging leaves, and in lateral root primordia (data not shown). It is possible that *ALC* is functionally redundant with other genes in regulating processes such as ovule development but is essential only for silique dehiscence. Double mutant analysis with other related myc/bHLH genes might be informative in this regard. We note that the dehiscence genes *SHP1* and *SHP2* also show expression in the developing gynoecium and ovules and also result in no obvious ovule defects when mutated [7].

SHP and *FUL* genes are expressed in the *alc* mutant

The MADS-box genes *SHP1*, *SHP2*, and *FUL* have been shown to regulate DZ formation. The transcripts of all three genes were detected in *alc* mutant siliques by RT-PCR (Figure 6b). This is consistent with the observation that silique expansion and lignification of the valve margin cells proceeds normally in *alc* siliques. The *alc* mutant phenotype, expression pattern, and the presence of *SHP1*, *SHP2* transcripts in homozygous *alc* plants suggest that *ALC* may act downstream to *SHP* genes or independently in a parallel pathway. The regulation of *ALC* by *SHP* can be further explored using plants that overexpress *SHP* genes or in *ful* mutant where *SHP1 SHP2* are ectopically expressed throughout the valves [9]. To investigate this possibility, we have recently constructed *alc ful* double mutant; preliminary studies show partial suppression of the *ful* phenotype by the *alc* mutation (our unpublished data).

Manipulation of fruit dehiscence in transgenic plants

Identification of *ALC* as a regulator of silique dehiscence has potential application to several crops, from legumes to oil seeds, especially where early dehiscence leads to significant yield losses, as in canola (*Brassica napus*) [19]. To test the possibility of engineering reduced shattering in crop plants through modification of the NLC layer, two approaches are being taken for the reduction of *ALC* activity in transgenic plants. We used both antisense RNA constructs and dominant-negative constructs [20]. The dominant-negative construct was made by replacing the basic domain of *ALC* protein with acidic amino acids. We recovered transgenic plants overexpressing either *ALC* antisense RNA or the dominant-negative *ALC* under the CaMV 35S promoter that showed defects in dehiscence (Figure 7f,g). Detailed characterizations of these transgenic lines are in progress. Unlike *shp1shp2* mutants or CaMV 35S -*FUL*, which block dehiscence by preventing the formation of the entire DZ, alteration of *ALC* function affects only a subset of cells within the DZ, with no changes in the external morphology of the silique. Consequently, the *alc* mutant siliques can be opened by simple manual pressure applied to the DZ, without requiring breakage of the fruit walls. Thus, our results provide a strategy to delay or block dehiscence through manipulation of the cell types within the DZ, which may provide advantages over approaches in which the DZ formation has been completely blocked.

Discussion

ALC is required for the formation of a nonlignified cell separation layer in the DZ

It has been proposed that, due to the restricted movement of plant cells, separation from neighboring cells is achieved by the formation of a morphologically distinct layer which is preprogrammed differently from adjacent nonseparating cells to undergo cell wall degradation [1]. Due to the relative accessibility of the tissues undergoing fruit dehiscence, anatomical investigations of cell separation during this process have been relatively detailed. The physiology of dehiscence at the DZ is well studied [21, 19, 22], but, due to the paucity of mutants, the functions of different cell layers in dehiscence have been speculative. The *alc* mutant is unusual in that it provides the first instance of a mutation that disrupts formation of a specific cell layer at the site of cell separation during dehiscence.

Detailed ultrastructural studies in *Brassica* by Meakin and Roberts [23] have shown that thin-walled cells, which are likely to correspond to the NLC layer in this study, occupy the site of separation during silique dehiscence. They have proposed that during dehiscence loss of cellular cohesion is due to degradation of cementing cell wall material resulting from the autolysis of these cells within the DZ [24]. The dissolution of cell walls is correlated with an increased activity of hydrolytic enzymes like cellulases, and the loss of plasma membrane integrity may allow access of these enzymes to the cell wall [24]. We can postulate that similarly, in *Arabidopsis*, the NLC layer undergoes autolysis and cell wall degradation to separate the valve from the replum. Since the NLC layer is absent in the *alc* mutant, we cannot directly assess whether the process of cell separation is primarily driven by autolysis or by cell wall degradation or if both are equally important. We have shown that loss of *ALC* function results in occupation of the site of separation by nonlignified replum-like cells at the outer margin and ectopic lignified cells toward the inner margin (Figure 4c). The *alc* mutant phenotype suggests that, even in the absence of a NLC layer, cells toward the outer valve margin can degrade. The cell separation observed at the outer valve margin in *alc* siliques is not as smooth as seen in wild-type, indicating that mechanical tearing rather than autolysis may be more responsible for the degradation of these cells, as siliques are under tension due to lignification. However, at the inner valve margin, ectopic lignification of cells makes them resistant to tension as well as enzymatic degradation, resulting in the attachment of the valves to the replum.

The dehiscence mechanism acts through a lignified/nonlignified sandwich

These observation show that, in addition to the well established importance of lignification, the presence of nonlignified cells at the boundary have an important role in fruit dehiscence. The mechanism of dehiscence can be viewed as a consequence of four major steps. The initial step is the differentiation of the DZ at the valve margins under the control of *SHP1/SHP2* genes as the silique grows after fertilization. Then, the lignification of inner valve layer and the LC layer of the DZ is needed to create tension within the fruit as the fruit desiccates and the outer valve cells shrink [6]. The *ALC* gene later promotes a subset of cells within the DZ, i.e., the NLC layer, to differentiate and subsequently form a nonlignified boundary between the valve margin and the replum. Lignification and NLC layer differentiation may be independent events, since the lignification of cells in the DZ is not perturbed in the *alc* mutant. Further, cell identity may be more important then cell position to prevent lignification of cells in the NLC layer, as the cells at the same position get ectopically lignified in *alc* mutants. In the final step toward dehiscence, the NLC layer eventually undergoes autolysis and cell wall degradation, possibly through induction of cell wall-degrading enzymes by the same cells. As these cells degrade, the existing tension within the fruit aids to separate the valves from the replum ensuing seed dispersal. Extensive lignification of the inner valve cells may be required for pod shattering, since crops such as *B. juncea* which have reduced lignification also show reduced shattering [6]. However, lignification of the cells at the inner valve margin as observed in *alc* mutants can block

dehiscence. Therefore, while lignification is necessary, the maintenance of nonlignified cells at the site of separation sandwiched between layers of lignified cells is apparently essential for dehiscence to be accomplished.

The mechanism of fruit dehiscence may be relevant to related processes such as abscission, anther dehiscence, as well as other processes in which cell separation is required. During abscission, shedding of organs occurs at anatomically distinct regions called "abscission zones" (AZ) [25]. Similar to DZ, AZ consists of a few layers of cells, but, during abscission, cell wall degradation is restricted to cells at the separation layer, which generally consist of small nonlignified cells [26]. Hence, premature abscission of various plant parts, like leaves, fruits, and flowers, in agronomically important crop plants might be prevented by genetic manipulation to alter the differentiation or lignification state of the cell layers within the abscission zone.

Materials and methods

Plant material and generation of the alc mutant

Generation of insertion lines in *Arabidopsis thaliana* carrying *Ds* gene trap was done according to Sundaresan et al. [10]. The *alc* mutation segregated in a 3:1 ratio when outcrossed to wild-type *Ler*, indicating that the mutation is recessive.

Molecular analysis

Isolation of flanking DNA at the insertion site was performed by TAIL-PCR [11] using the *Ds*-specific primers and conditions described in [27]. Primers were designed from the BAC sequence surrounding the *Ds* insertion site and used to amplify a product from an *Arabidopsis* floral cDNA library (constructed by Detlef Weigel) obtained courtesy of the *Arabidopsis* Biological Resource Center. The PCR fragment obtained was sequenced and used as a probe to screen the same library, using standard techniques [28]; 11 positive cDNA clones were isolated and sequenced.

RT-PCR analysis and 5′ RACE

All RT-PCR was performed using the Qiagen One Step RT-PCR kit on total silique RNA isolated using the RNeasy plant mini-kit (Qiagen). *SHP1*, *SHP2*, and *FUL* gene expression in *alc* background was detected using respective gene-specific primers. The 5′RACE was performed according to the Boehringer Mannheim 5′/3′ RACE Kit, using briefly 2 μg of total RNA from wild-type *Arabidopsis* inflorescence for first-strand cDNA synthesis. The 5′cDNA RACE products were gel purified and sequenced.

Characterization of Ds insertion site and reversion analysis

The *Ds* insertion site was analyzed by sequencing using *ALC*-specific primer ALC 1 (TCTCTAGGTTCAGGTCTTGCT) and ALC 4 (TCAC CACCGAAGAGTACTA) and the *Ds* primers. For reversion, homozygous *alc* plants were crossed to homozygous *Ac* carrying plants, and, in the F2 generation, plants homozygous for *alc* were screened for somatic reversion of the mutant phenotype to wild-type. Footprint analysis of the revertant plants was performed by PCR using ALC 1 and ALC 4 primers, which span the *Ds* insertion site and products sequenced.

Microscopy and histological staining

Siliques were fixed in historesin and sectioned. Staining for β-glucuronidase expression in tissues was done as described in Sundaresan et al. [10]. Lignin analysis was performed according to Liljegren et al. [7].

Scanning and transmission electron microscopy

SEM was performed on fresh siliques mounted on silver tape, frozen in liquid nitrogen, and viewed using Joel JSM-5310 LV microscope. For TEM, siliques from wild-type and *alc* plants were fixed and prepared according to Barnes et al. [29], with slight modification [30].

Generation of the dominant-negative construct

The dominant-negative construct was made by deleting amino acids from number 90 to 106 in the *ALC* cDNA and replacing them by acidic residues coded by the sequence GAAGAGGAAGACGATGAAGAG GAT by a two-step PCR approach.

Supplementary material

Details of RT-PCR, cloning of dominant-negative construct, transformation [31], and TEM are available as Supplementary material with this article online at http://images.cellpress.com/supmat/supmatin.htm.

Acknowledgements

We are grateful to S. Parinov, S. Mayalagu, and S. Thanumalayan for their help and advice with TAIL-PCR; and to C. Yang Sun and L. Cheng Wen for assistance with SEM and TEM. We thank M. Griffith, Y. Wei Cai, D. Smyth, and M. Yanofsky for helpful suggestions and comments on the manuscript. This research was funded by grants from the National Science and Technology Board of Singapore.

References

1. Roberts JA, Whitelaw CA, Gonzalez-Carranza ZH, McManus MT: **Cell separation processes in plants–models, mechanisms and manipulation.** *Ann Bot* 2000, **86:**223-235.
2. Sessions A: **Piecing together the *Arabidopsis* gynoecium.** *Trends Plant Sci* 1999, **4:**296-297.
3. Bowman JL, Baum SF, Eshed Y, Putterill J, Alvarez J: **Molecular genetics of gynoecium develpoment in *Arabidopsis*.** *Curr Top Dev Biol* 1999, **45:**155-205.
4. Ferrandiz C, Pelaz S, Yanofsky MF: **Control of carpel and fruit development in *Arabidopsis*.** *Ann Rev Biochem* 1999, **68:**321-354.
5. Smyth DR, Bowman JL, Meyerowitz EM: **Early flower development in *Arabidopsis*.** *Plant Cell* 1990, **2:**755-767.
6. Spence J, Vercher Y, Gates P, Harris N: **Pod shatter in *Arabidopsis thaliana*, *Brassica napus* and *B. juncea*.** *J Microsc* 1996, **181:**195-203.
7. Liljegren SJ, Ditta GS, EshedY, Savidge B, Bowman JL, Yanofsky MF: **Shatterproof MADS-box genes control seed dispersal in *Arabidopsis*.** *Nature* 2000, **404:**766-770.
8. Gu Q, Ferrandiz C, Yanofsky MF, Martienssen R: **The *FRUITFULL* MADS-box gene mediates cell differentiation during *Arabidopsis* fruit development.** *Development* 1998, **125:**1509-1517.
9. Ferrandiz C, Liljegren SH, Yanofsky MF: **Negative regulation of the *SHATTERPROOF* genes by *FRUITFULL* during *Arabidopsis* fruit development.** *Science* 2000, **289:**436-438.
10. Sundaresan V, Springer P, Volpe T, Howard S, Jones JDG, Dean C, *et al.*: **Patterns of gene action in plant development revealed by enhancer trap and gene trap transposable elements.** *Genes Dev* 1995, **9:**1797-1810.
11. Liu YG, Mitsukawa N, Oosumi T, Whittier RF: **Efficient isolation and mapping of *Arabidopsis thaliana* T-DNA insert junctions by thermal asymmetric PCR.** *Plant J* 1995, **8:**457-463.
12. Altschul SF, Gish W, Miller W, Myers EW, Lipman DJ: **Basic local alignment search tool.** *J Mol Biol* 1990, **215:**403-410.
13. Heisler MGB, Atkinson A, Bylstra YH, Walsh R, Smyth DR: ***SPATULA*, a gene that controls development of carpel margin tissues in *Arabidopsis*, encodes a bHLH protein.** *Development* 2001, **128:**1089-1098.
14. Ni M, Tepperman JM, Quail PH: **PIF3, a phytochrome-interacting factor necessary for normal photoinduced signal transduction, is a novel basic helix-loop-helix protein.** *Cell* 1998, **95:**6557-6667.
15. Ludwig SR, Wessler SR: **Maize R gene family tissue-specific helix-loop-helix proteins.** *Cell* 1990, **62:**849-852.
16. Goff SA, Cone KC, Chandler VL: **Functional analysis of the transcriptional activator by the maize B gene: Evidence for a direct functional interaction between two classes of regulatory proteins.** *Genes Dev* 1992, **6:**864-875.

17. Abe H, Yamaguchi-Shinozaki K, Urao T, Iwasaki T, Hosokawa D, Shinozaki K: **Role of *Arabidopsis* MYC and MYB homologs in drought- and abscisic acid-regulated gene expression.** *Plant Cell* 1997, **9:**1859-1868.
18. Kay SA: **PAS, present and future: clues to the origins of circadian clocks.** *Science* 1997, **276:**753-754.
19. Jenkins ES, Paul W, Coupe SA, Bell SJ, Davies EC, Roberts JA: **Characterization of a mRNA encoding a polygalacturonase expressed during pod development in oilseed rape (*Brassica napus* L.).** *J Exp Bot* 1996, **47:**111-115.
20. Krylov D, Kasai K, Echlin DR, Taparowsky EJ, Arnheiter H, Vinson C: **A general method to design dominant negatives to B-HLHZip proteins that abolish DNA binding.** *Proc Natl Acad Sci USA* 1997, **94:**12274-12279.
21. Coupe SA, Taylor JE, Issac PG, Roberts JA: **Characterization of a mRNA that accumulates during development of oilseed rape pods.** *Plant Mol Biol* 1994, **24:**223-227.
22. Child RD, Chauvaux N, John K, Ulvskov P, Van Onckelen HA: **Ethylene biosynthesis in oilseed rape pods in relation to pod shatter.** *J Exp Bot* 1998, **49:**829-838.
23. Meakin PJ, Roberts JA: **Dehiscence of fruit in oilseed rape (*Brassica napus* L.) 1. Anatomy of pod dehiscence.** *J Exp Bot* 1990, **41:**995-1002.
24. Meakin PJ, Roberts JA: **Dehiscence of fruit in oilseed rape (*Brassica napus* L.) 2. The role of cell wall degrading enzymes and ethylene.** *J Exp Bot* 1990, **41:**1003-1011.
25. van Doorn WG, Stead AD: **Abscission of flowers and floral parts.** *J Exp Bot* 1997, **48:**821-837.
26. Sexton R: **Cell biology of Abscission.** *Ann Rev Plant Physiol* 1982, **33:**133-162.
27. Grossniklaus U, Vielle-Calzada J-P, Hoeppner MA, Gagliano WB: **Maternal control of embryogenesis by *MEDEA*, a *polycomb* group gene in *Arabidopsis*.** *Science* 1998, **280:**446-450.
28. Sambrook J, Fritsch EF, Maniatis T: *Molecular Cloning: A Laboratory Manual*, 2nd edn. Cold Spring Harbor, NY: Cold Spring Harbor Press. 1989.
29. Barnes SA, Nishizawa NK, Quaggio RB, Whitelam GC, Chua NH: **Far-red light blocks greening of *Arabidopsis* seedlings via a phytochrome A-mediated change in plastid development.** *Plant Cell* 1996, **8:**601-615.
30. Spurr AH: **A low- viscosity epoxy resin embedding medium for electron microscopy.** *J Ultrastruc Res* 1969, **26:**31-43.
31. Clough SJ, Bent AF: **Floral dip: a simplified method for Agrobacterium-mediated transformation of *Arabidopsis thaliana*.** *Plant J* 1998, **16:**735-743.
32. Urao T, Yamaguchi-Shinozaki K, Urao S, Shinozaki K: **An *Arabidopsis myb* homolog is induced by dehydration stress and its gene product binds to the conserved MYB recognition sequence.** *Plant Cell* 1993, **5:**1529-1539.
33. Radicella JP, Turks D, Chandler LV: **Cloning and nucleotide sequence of a cDNA encoding B-Peru, a regulatory protein of the anthocyanin pathway in maize.** *Plant Mol Biol* 1991, **17:**127-130.
34. Ludwig SR, Habera LF, Dellaporta SL, Wessler SR: ***Lc*, a member of the maize R gene family responsible for tissue-specific anthocyanin production, encodes a protein similar to transcriptional activators and contains the myc-homology region.** *Proc Natl Acad Sci USA* 1989, **86:**7092-7096.